Journal of Applied Polymer Science

Study the Factors Affecting the Performance of Organic–Inorganic Hybrid Coatings

Weili Li,[1] Dong Huang,[1] XinYu Xing,[1] Jijun Tang,[1] Yujin Xing,[1] Xiujuan Li,[1] Jide Zhang[2]

[1]School of Material Science and Engineering, Jiangsu University of Science and Technology, Zhenjiang 212003, China

[2]Key Laboratory of Green Packaging and Biological Nanotechnology, Hunan University of Technology, Zhuzhou 412007, China

Correspondence to: W. Li (E-mail: just_liweili@163.com) and J. Zhang (E-mail: 401522267@qq.com)

ABSTRACT: In this article, a series of hybrid organic–inorganic coatings based on silica-epoxy composite resins were prepared with the sol-gel method by using γ-aminopropyl triethoxysilane as a coupling agent. Especially, the research emphasized on the factors that influenced on the properties of the prepared hybrid coatings. Firstly, epoxy resin was reacted with γ-aminopropyl triethoxysilane at a specific feeding molar ratio; subsequently, the asprepared sol–gel precursor was cohydrolyzed with tetraethoxysilane (TEOS) at various contents to afford chemical bondings to form silica networks and give a series of organic–inorganic hybrid coatings. They were loaded and cured on steel panels and characterized for FTIR, TGA, DSC, water contact angles (WCA), pencil hardness, surface & three-dimensional morphological studies, and potentiodynamic polarization tests. The surfaces of the hybrid coatings showed Sea-Island or Inverting Sea-Island morphologies at a certain relative content of two components, which made the coatings possess hydrophobic property. Due to the contribution of organic and inorganic components, the prepared hybrid coatings possess a lot of properties such as pencil hardness, thermotolerance, and corrosion resistance. © 2014 Wiley Periodicals, Inc. J. Appl. Polym. Sci. **2014**, *131*, 41010.

KEYWORDS: coatings; mechanical properties; morphology; thermal properties

Received 26 December 2013; accepted 12 May 2014

DOI: 10.1002/app.41010

INTRODUCTION

Organic–inorganic hybrid materials have received considerable attention as new functional materials. It represents a natural interface between two worlds of chemistry (organic and inorganic), and the main idea of developing hybrid materials is to take advantage of the best properties of each components (the polymeric material and the ceramic powder) forming the hybrid and try decreasing or eliminating their drawbacks and getting in an ideal way to synergic effect.[1] The recent reviews by Zheludkevich et al.,[2] Wang and Bierwagen[3] gave an exhaustive account of the research that had been carried out so far on applicability of sol–gel coatings on metals and alloys for corrosion protection.

Generally, the hybrid material is formed through the hydrolysis and condensation of organically modified silicates with traditional alkoxide precursor.[4,5] For the hybrid materials, silicon alkoxides are frequently used as sol–gel precursors, which function as both corrosion inhibitors and adhesion promoters. Organofunctional group like silane-coupling agent is necessary for adhesion promoter application between different phases. For example, Karataş et al.[6] studied a series of UV-cured organic–inorganic hybrid coating materials, in which, methacryloxypropyltrimethoxy silane (MAPTMS) was used as a silane-coupling agent to improve the compatibility of organic and inorganic phases. Yeh et al.[7] studied a series of sol–gel-derived organic–inorganic hybrid coatings consisting of organic poly(methyl methacrylate)(PMMA) and inorganic silica(SiO_2) by using 3-(trimethoxysilyl) proply methacrylate (MSMA) as a coupling agent. Trabelsi et al.[8] studied organic–inorganic coatings which were synthesized from tetraethoxysilane (TEOS) and vinyltriacetoxysilane (VTAS) via dual process involving sol–gel reaction and radical polymerization.

A lot of researchers have concentrated on the influence of silane-coupling agent on the prepared hybrid coatings. However, the properties of the hybrid materials are mainly determined by their major constituents, e.g., organic and inorganic components, and they play different role in the system. The result of Ouissem Trabelsi[8] confirmed that thermally cured hybrid material formed a uniform, homogenous and defect-free thin film on copper substrates. Thermal stability increased with the content of silica in the starting precursors of the hybrid system, and the increase of the amount of organic constituents in the hybrid network led to an important decrease in the hardness

Table I. Compositions of the Prepared Hybrid Coating

Organic–inorganic hybrid coatings	Modified epoxy resin (g/mL)	TEOS (g/mL)
I(MEp/HSi = 9 : 1)	0.454	0.046
II(MEp/HSi = 7 : 3)	0.359	0.141
III(MEp/HSi = 5 : 5)	0.261	0.239
IV(MEp/HSi = 3 : 7)	0.159	0.341
V(MEp/HSi = 1 : 9)	0.054	0.446

and elastic modulus of the resulting films. As there are a lot of significant differences between organic part and inorganic part in the hybrid coatings, which will lead to diverse properties for the prepared hybrid coatings varied with the relative content of the two parts. Subasri et al.[9] used hexamethyldisilazane (HMDS) as an organic modifying agent to prepare nonfluorinated hydrophobic silica coatings. Incorporation of low surface energy organic functional groups helped the surface of the hybrid coating material possess hydrophobic characteristics and good corrosion resistance.

Besides, microstructure of the coating surface is the other factor which influences the properties of the hybrid coatings. The self-cleaning property of lotus leave is provide by the special structure and low free energy material on the surface where are micropapillae with diameters ranging from 5 to 9 μm and branch-like nanostructure with average diameters of 124 nm on both the top of micropapillae and area between micropapillae.[10] Inspired by the lotus leaves phenomenon, many methods have been developed to construct dual-size rough structure in order to fabricate self-cleaning surface, such as assembling silica micro- and nanosphere via electrostatic absorbing and template directed self-assembly,[11] lotus-like aligned carbon nanotube film via chemical vapor deposition,[10,12] nanoflower on metal via wet chemical etching,[13] film with microsphere/nanofiber composite structure via electronspinning,[14] porous structure on polymer surface via microphase separation of polymer in selective solvents,[15–17] organosilicon foams via sol–gel phase separation.[18,19]

In the present study, to evaluate the factors which influence the properties of the organic–inorganic hybrid coatings systematically, a series of organic–inorganic hybrid coatings were prepared by means of sol–gel reaction. The microstructure of the hybrid materials were observed carefully, and the factors which influence the properties of the prepared hybrid coatings such as mechanical, hydrophobical, thermal and anticorrosion properties were investigated carefully.

EXPERIMENTAL

Materials

Tetraethoxysilane (TEOS,Alfa,99%) and γ-aminopropyl triethoxysilane (Aldrich,96%), diglycidyl ether of biphenol A type epoxy resin (epoxy equivalent, 500 g/Eq, Jiangsu SanMu Group, China) were all commercial reagents. All other organic solvents, such as ethanol, butanol, and xylene, were analytical reagents and directly used without purity.

Preparation of the Organic–Inorganic Hybrid Precursor Material

The hybrid precursor materials were prepared by sol–gel process in two steps. At first, epoxy resin was blended with γ-aminopropyl triethoxysilane in mixed solution of ethanol/butanol/xylene = 1/1/1(by volume) under continuous stirring at 80°C for 2 h. During this reaction, epoxy group would react with amino group at molar ratio of 1 : 1. Then, a quantity of TEOS was added into the product of Step 1 followed by introduction of H_2O at molar ratio of H_2O : Si = 4 : 1. A catalytic amount of acetic acid was then added into the solution and the reaction was continued for 72 h at 25°C in acidic conditions. After completion of reaction, the solution became viscous to form a gelatinous state.

Coating Procedure

Four sheets of steel panels (one 150 × 70 × 1.0 mm^3 for potentiodynamic polarization curves analysis, and three 120 × 50 × 0.5 mm^3 for water contact angles of film surfaces, pencil scratch hardness, and optical microscope observation) were prepared and subjected to pretreatment of the following steps: polishing using metallographic sand paper, alkaline washing for removing grease, acid polishing, and drying. For coating, the pretreated steel panels were dipped into the coating solution at a speed of 200 mm/min using a specially designed apparatus. After dipping, the coated samples were dried and cured in an oven at 80°C for 6 h. The coating procedure was repeated for many times until the prepared complete coating without a pinhole on the surface. The thick of each coatings were controlled around 80–100 μm, which was detected by Coating Thickness Gauge (Leeb250, Shanghai Modern Environmental Engineering Technology). In order to unify the experimental conditions, the mixed mass concentration of modified epoxy resin and TEOS is fixed to 0.5 g/mL. In addition, to study the influence of the relatively content of organic–inorganic components on the micromorphologies and properties of the prepared hybrid coatings, the relative mol ratio of epoxy group for modified epoxy resin(-short for MEp) to Silicone group for hydrolized TEOS(short for HSi) was varied at the proportion of 9/1(Sample I), 7/3(Sample II), 5/5(Sample III), 3/7(Sample IV), and 1/9(Sample V), respectively. Table I summarizes the mass concentration of the reagents for different hybrid coating samples, and Scheme 1 presents the synthetic route for the organic–inorganic hybrid coating.

Characterization

FTIR measurements were carried out on BRUKER VECTOR-22 spectrometer at room temperature. The spectra were collected over the range 400–4000 cm^{-1} by averaging 128 scans at a maximum resolution of 2 cm^{-1}.

Pencil scratch hardness of the coatings were measured according to ASTM D 3363-05. A coated panel was placed on a firm horizontal surface. The pencil was held firmly against the film at a 45° angle (point away from the operator) and pushed away from the operator in a 6.5-mm (1/4-in.) stroke. The process was started with the hardest pencil and continued down the scale of hardness to either of two end points: one, the pencil that will not cut into or gouge the film (pencil hardness), or

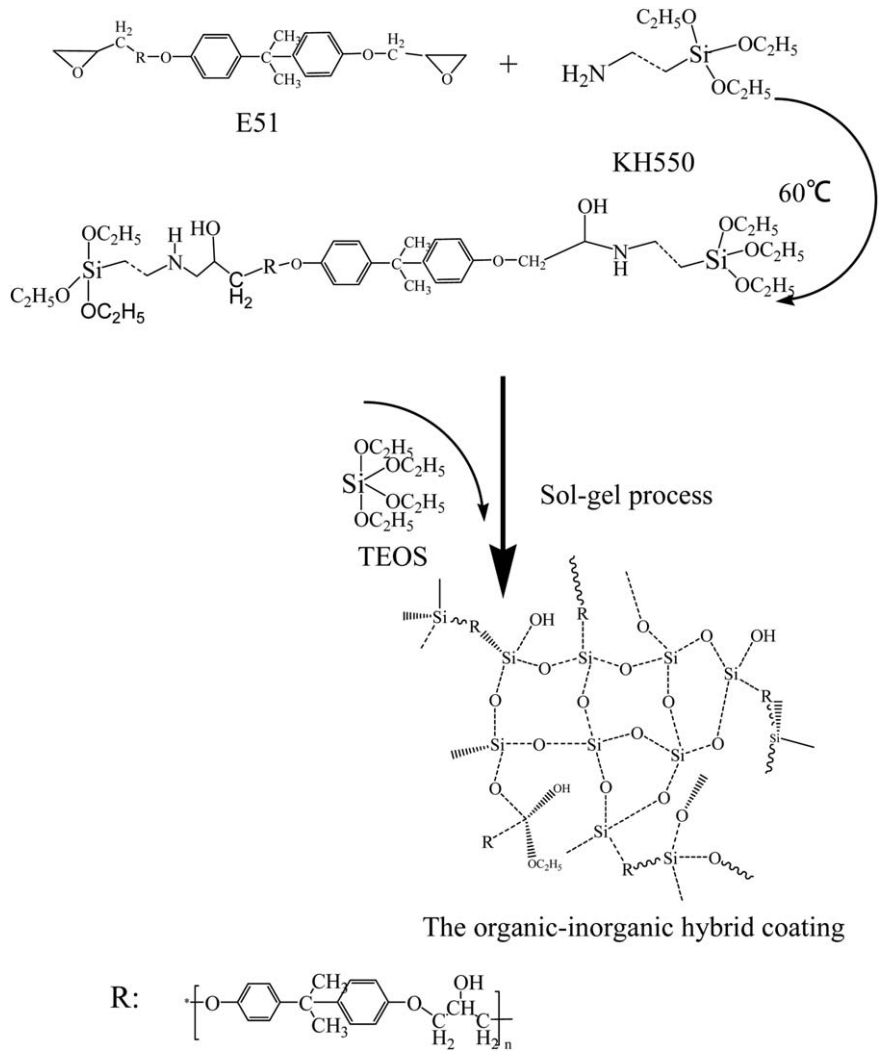

Scheme 1. Synthetic route for the organic–inorganic hybrid coating.

two, the pencil that would not scratch the film (scratch hardness).

Water contact angles (WCA) were measured by using a Drop Shape Analyzer (DSA)(JC2000D, Powereach Corporation, Shanghai, China). The volume of water droplet was ~4 μL and the averages of 10 measurements were reported as the water contact angle.

The surface morphologies of the hybrid organic–inorganic coatings were assessed using 3D measuring laser microscope (OLS4000, Olympus Corporation).

Thermal degradation behavior of the hybrid organic–inorganic coatings was investigated with a TA Instruments (TGA Q500) from room temperature to 1000°C under nitrogen atmosphere at heating rate of 10°C/min. The measurements were conducted with 10–20 mg samples. During heating period, the weight loss and temperature difference were recorded as a function of temperature.

DSC measurements were carried out using DSC Q100 (TA Instruments) over the temperature of 20–200°C at a scan rate of 10°C/min. All the thermograms were baseline corrected and calibrated using Indium metal. The experimental specimens (8–10 mg) were dried at 60°C under vacuum for 24 h before being measured. All the samples were first annealed at 120°C for 3 min, and cooled to 20°C using liquid nitrogen and then scanned for the measurement.

Corrosion analyses for bare and coated substrates were done using a dual unit electrochemical workstation (CS2350) (Wuhan Corrtest Instrument) connected to a corrosion analysis software program. Prior to the measurement, each sample was immersed in 3.5 wt % NaCl solution at least 30 min. Coated steel panels was exposed to a hole of 10 mm in diameter through which the caustic solution was in contact at room temperature during polarization tests. Saturated calomel was used as reference electrode (SCE) and a platinum sheet as counter electrode. The potentiodynamic measurements were taken between −500 mV and 1500 mV and versus SCE at a rate of 2.5 mV/s.

RESULTS AND DISCUSSION

Chemical Structure

Figure 1(a) shows the FTIR spectra for the prepared organic–inorganic hybrid coatings. They show similar absorption peaks

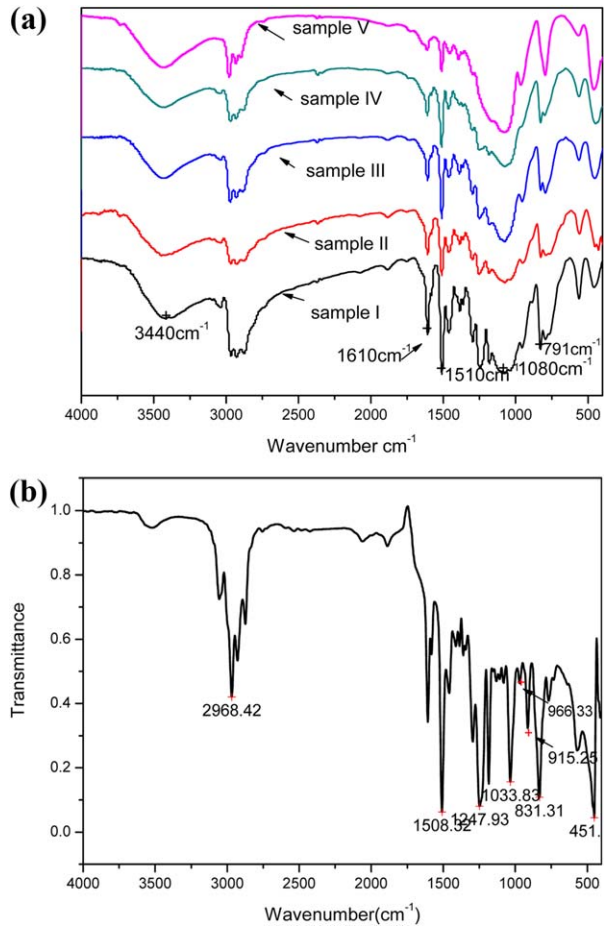

Figure 1. (a) FTIR spectra for the hybrid coatings. (b) FTIR spectrum for epoxy resin. [Color figure can be viewed in the online issue, which is available at wileyonlinelibrary.com.]

as expected, characteristic absorption peaks at 3440 cm^{-1} ($\nu_{Si\text{-}OH}$),[20] 2980 cm^{-1} ($\nu_{C\text{-}H}$), 1610 cm^{-1} ($\nu_{Ph\text{-}H}$), 1510 cm^{-1} ($\nu_{ar,C\text{-}C}$), 1080 cm^{-1} ($\nu_{as,Si\text{-}O\text{-}Si,}$), 791 cm^{-1} ($\nu_{sy,Si\text{-}O\text{-}Si}$)[21] can be seen from them, and the relative strength of absorption peaks for different functional groups are varied with the relative content of two components. In addition, the disappearing absorption peaks in the range from 950 cm^{-1} to 810 cm^{-1} for epoxy group, as can be seen from Figure 1(b), means that epoxy resin has reacted with γ-aminopropyl triethoxysilane and is joined to the silica sol by chemical bond.

Surface and Three-Dimensional Morphological Studies

For the organic–inorganic hybrid coatings, it is very important to explicit how the interaction of two components will impact on the surface morphology of the coating. A 3D measuring laser microscope uses laser scanning to perform non-contact 3D measurement of complex surface features of the samples. It guarantees both repeatability and accuracy, while also being capable of high-resolution observation and highly accurate measurement over a wider area. In addition, it also features easier operation, including a function for acquiring 3D images automatically with a single click. Optical images of the surfaces and three-dimensional morphologies for the organic–inorganic hybrid coatings are presented in Figures 2 and 3, respectively. Because hydrolysis and condensation of TEOS under acidic condition favor the formation of small particles in nanometer scale, ordinary TEOS-based inorganic coating tends to crack after it is cured[22]. However, due to the extensibility property of the blending organic components, no cracks were observed for the prepared hybrid coatings. In addition, it should be noted that with chemical connection of silane coupling agent(γ-aminopropyl triethoxysilane), organic and inorganic components are uniform distributed in the whole hybrid coatings, and the microstructure of the coating surfaces vary with the changed relative content of two components. For samples I and II, when the organic component is in the major, inorganic silica aggregate and present as particles in micrometer scale, which are surrounded by modified epoxy resin, and the surface present Sea-Island Morphology, the size and the content of silica particles increase with the content of inorganic component. However, when the content of the organic component and inorganic component is in equal, such as Sample III, the modified epoxy resin cannot encapsulate the inorganic component well and silica particles aggregate together to form as a whole, thanks to the interconnect function of silane coupling agent, the coating surface presents flat and uniform, it does not present phase splitting. With the content of inorganic component continue increases (for the hybrid coatings IV and V), the coating surfaces present Inverse Sea-Island Morphologies. In this stage, modified epoxy resin present as particles in micrometer scale and surrounded by the inorganic silica phases.

Physical and Static Contact Angle Measurements

Thermal stability of the prepared organic–inorganic hybrid coatings were determined by using TGA analysis. The thermograms for different hybrid coatings are given in Figure 4, and the weight losses with the increased temperature for different samples are summarized in Table II. When the organic components are in the major amounts, there are two major weight losses for the coatings beyond 250°C. For the first step, the loss can probably be owing to the dehydroxylation of water.[23] With the temperature increasing, the loss for the second step is attributed to the decomposition and disappearance of amino opened epoxy groups and other organic entities. When the content of inorganic component is higher, there are some differences for their mass losses from room temperature to 200°C, which may probably be attributed to the dehydration of the sample, such as the release of bound water, the absorbed water or ethanol from mesopores of the silica gel hybrids and the by-products of organo alkoxysilane compounds (i.e., acetic acid which has not been fully removed after being heated).[24] For all the samples, when the temperature exceeds 700°C, the residual inorganic part SiO_2 can still protect the metal properly at such high temperature. As epoxy resin is modified by silane coupling agent(γ-aminopropyl triethoxysilane), which can also convert to SiO_2 at a high temperature, so the residual SiO_2 is larger than the reactant ratio as listed in Table I.

Due to the interaction between organic and inorganic components, relative content between them may also impact on the polymer chains' movements. As is seen from the results of DSC (Figure 5 and Table III), there are no crystal-melting peaks for the prepared organic–inorganic hybrid coatings, which indicate that all the coatings present amorphous states. In addition, there is a glass transition temperature around 100°C which is attributed to the segmental motion of the modified epoxy resin,

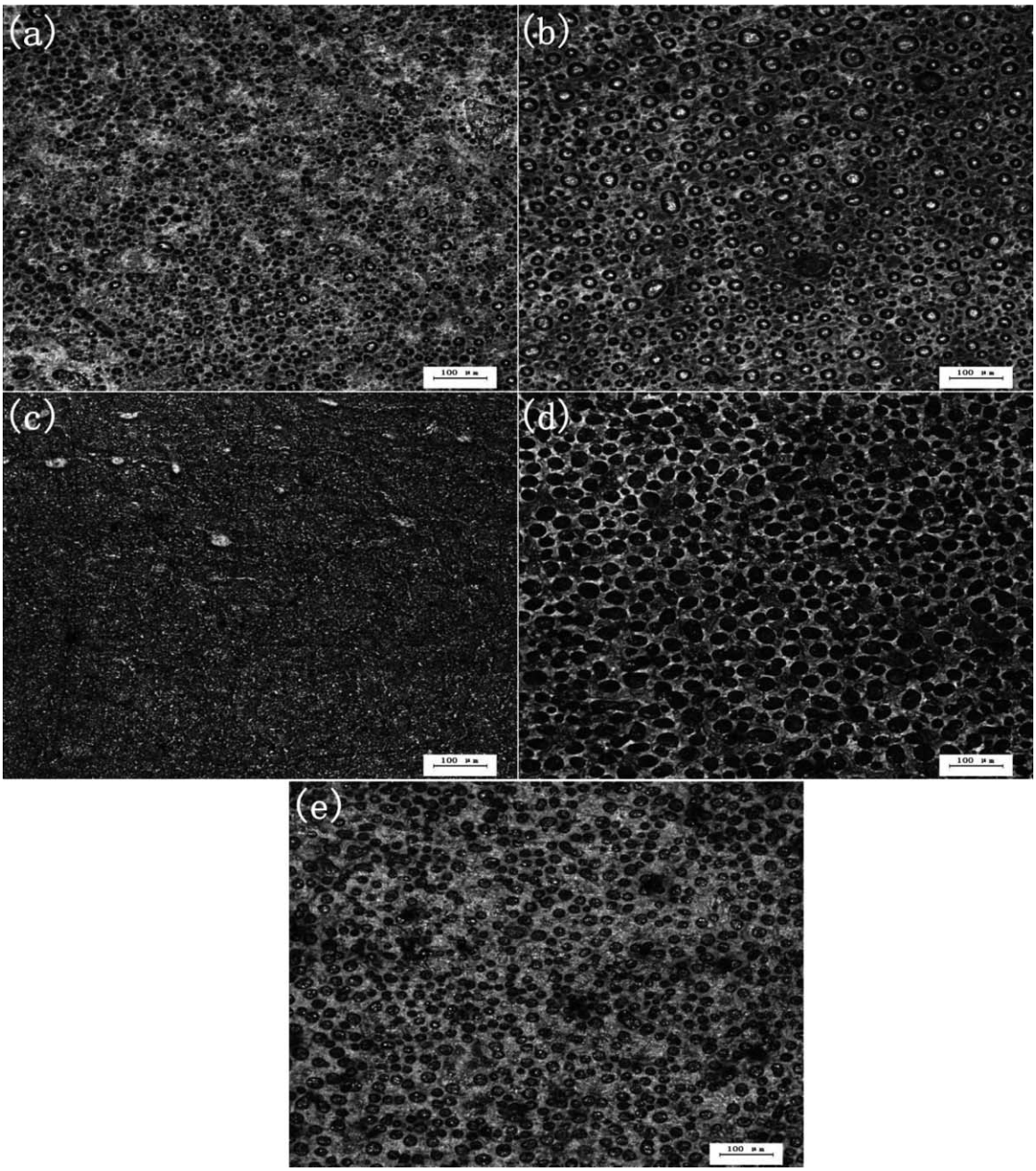

Figure 2. Optical images of the surface of hybrid coatings (a) Sample I; (b) Sample II; (c) Sample III; (d) Sample IV; (e) Sample V.

and it is increased with the content of inorganic component. As we know, there are a lot of silanols in the inorganic component, they can connect to the modified epoxy resin with covalent bond by sol–gel reaction; in addition, the unreacted silanols can also influence the organic component by hydrogen bond. With the restrict effect of silanols, the value of T_g for the modified epoxy resin will increase with the content of inorganic components.

For the hybrid coating system, the balance between the relative content of organic and inorganic components is important to achieve good barrier property while maintaining desirable mechanical performance. Depending upon its chemical structure, the organic constituent provides flexibility, hydrophobicity and reduces defects for the coating matrix. The inorganic part is responsible for the hardness of the coating, the superior adhesion to the metal surface and the heat resistance of the coating.[25] The samples were characterized by being deposited onto pretreated steel panels. The behaviors of the WCA and pencil scratch hardness for the organic–inorganic hybrid coatings are summarized in Table IV.

Contact angle is an important parameter to evaluate the surface of hybrid coating. It is well known that roughness enhances

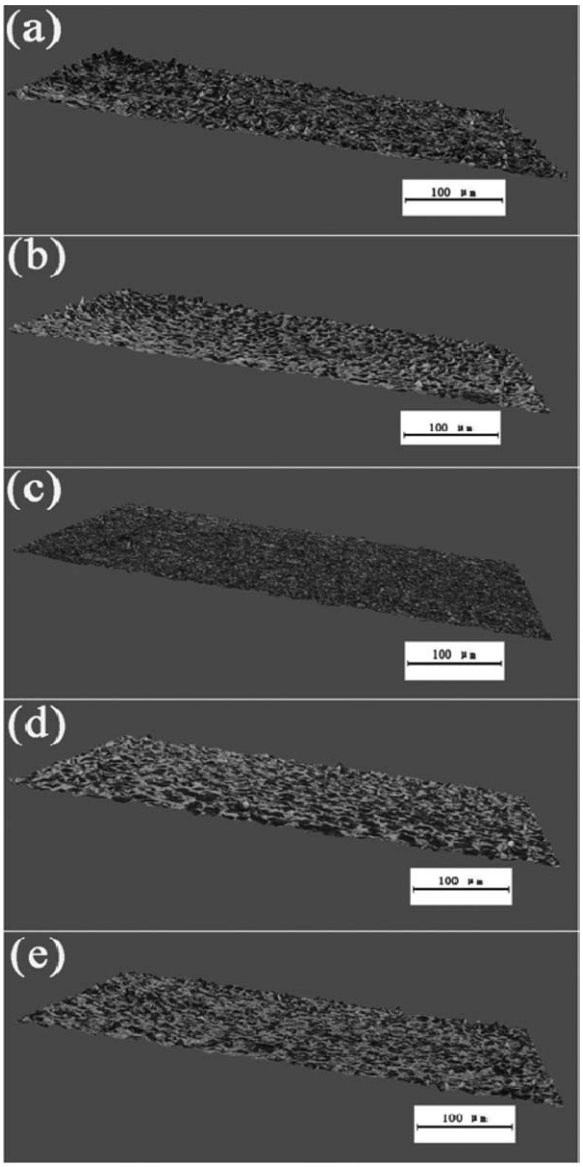

Figure 3. Optical images of three-dimensional shape of prepared hybrid coatings (a) Sample I; (b) Sample II; (c) Sample III; (d) Sample IV; (e) Sample V.

both hydrophobicity and hydrophilicity depending on the nature of the corresponding flat surface. Conradi et al. had prepared nanosilica-filled epoxy-resin composite coatings, It was found that a significant increase in the roughness for the epoxy coating with the embedded silica particles, which will increase the contact angle from 84.6° to 94.2°.[26] It suggests that micro-rough morphologies on the surface of the hybrid coatings makes them have hydrophobic property.

As is expected, the hybrid coating (Sample III) shows the lowest contact angle of a water droplet ($98 \pm 2°$) due to its flat surface. However, it is still higher than the pure silica coating ($74 \pm 3°$).[27] In previous studies, it was demonstrated that the precursors of silica coatings were usually hydrophilic, and became wet under the conditions of atmospheric moisture and water.[26] The hydroxyl groups present on the hydrophilic silica coating surface are the major sources of hydrophilicity as they promote the adsorption of water. Terminal hydroxyl groups which can interact with water, lead to deterioration of the silica network.[27] Therefore, with appropriate surface chemical modification, e.g., some of the silanol groups on the hybrid coating surface are replaced by epoxy groups, the surface can be rendered hydrophobic so that the water molecule will be repelled. The contact angle of a water droplet on the organic–inorganic hybrid coating increases when the precursor with the hydrophobic organic group is added into the hybrid coatings.[28] In this way, hydrophobic surfaces could be achieved.

The wettability of the coating surface is not only dependent on its chemical composition, but also on its topography.[29,30] The surfaces of the hybrid coatings (I, II, IV, V) present Sea-Island or Inverse Sea-Island Morphologies in μm scale (as can be seen from Figures 2 and 3) and this effect ensure that the contact area which is available to water is very low and this will prevent the penetration of water. The net result is that the water contact angles for these hybrid coatings increases significantly, and the cured hybrid coatings present superhydrophobicity property.

Mechanical property is another factor to evaluate the prepared hybrid coating. Table II shows the result of pencil hardness for the hybrid coatings. From the result, inorganic hydrolyzed silica component contributes to the hardness of the coatings, and the scratch hardness for the hybrid coatings increase with its content. Although the bond length of Si-O is longer than that of ordinary organic bond (C-C or C-O), the crosslinked structure after sol–gel reaction will restrain the chain's movement, in addition, the effect of hydrogen bonding from the retained silanol can also enhance the hardness of the resultant organic–inorganic hybrid coatings.

Potentiodynamic Polarization Tests

Figure 6 shows the result of the polarization curves of steel panels coated by a serious of hybrid coatings and the bare samples, and the electrochemical parameters obtained from the potentiodynamic polarization curves are listed in Table V.

The potentiodynamic polarization of bare steel panel's substrate exhibits no obvious passivation region and the current density

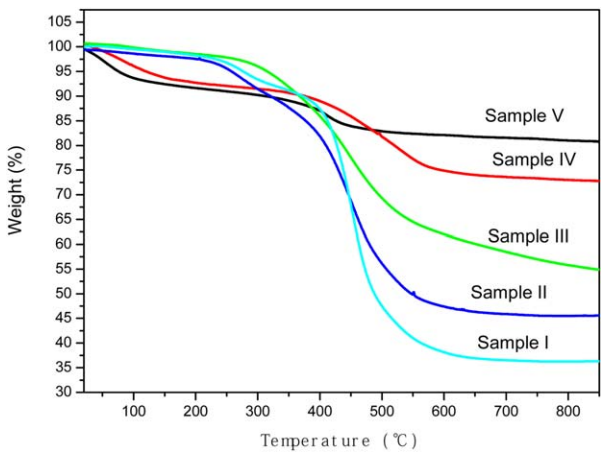

Figure 4. TGA analysis for the hybrid coatings. [Color figure can be viewed in the online issue, which is available at wileyonlinelibrary.com.]

Table II. Weight Losses for Different Hybrid Coatings at Different Temperature

Sample / Temperature	100°C	200°C	300°C	400°C	500°C	600°C	700°C	800°C
Sample I	99.5%	98.26%	93.38%	87.39%	47.34%	38.13%	36.52%	36.26%
Sample II	98.6%	97.55%	91.43%	81.87%	56.12%	47.40%	45.89%	45.50%
Sample III	99.8%	98.53%	96.03%	85.92%	69.30%	62%	58.49%	55.80%
Sample IV	96.1%	92.73%	91.84%	89.00%	81.78%	74.89	73.61%	72.99%
Sample V	93.67%	91.64%	90.28%	87.06%	82.87%	82.11%	81.54%	81.00%

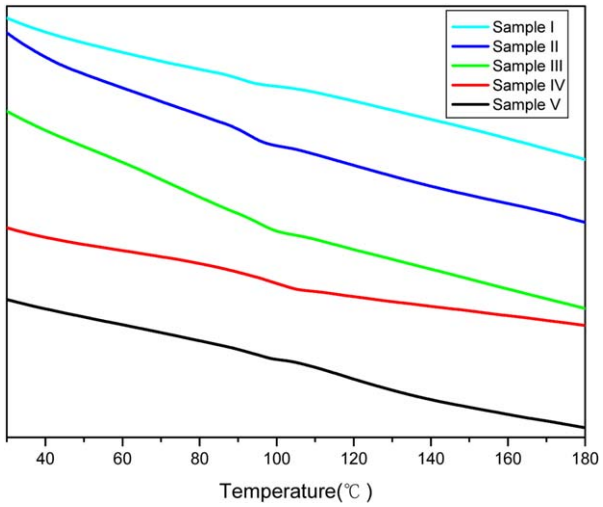

Figure 5. DSC measurements for the hybrid coatings. [Color figure can be viewed in the online issue, which is available at wileyonlinelibrary.com.]

initially increases rapidly above its open circuit potential because an active electrochemical reaction has occurred on the surface. However, lower I_{corr} values for the organic–inorganic hybrid coatings compare to the bare substrate indicates that coatings indeed can provide a physical barrier for blocking the electrochemical process. As can be seen from optical microscope, the surface of hybrid coating III shows flat and uniform. With the properties of good wet-adhesion and barrier effect of dense structure, the corrosive medium such as water, oxygen and salt, cannot pass through the hybrid coating to corrode the protected metal. The hybrid coating (III) shows the best

Table III. The Value of Glass Transition Temperature for Different Hybrid Coatings

Sample	T_g (°C)
I	90.81
II	92.73
III	95.77
IV	98.34
V	111.84

Table IV. Physical Properties and Contact Angle Values of the Obtained Coatings

	Coating properties	
Organic–inorganic hybrid coatings	WCA (°)	Pencil scratch hardness
I (MEp/HSi = 9/1)	120 ± 2	HB
II (MEp/HSi = 7/3)	135 ± 2	H
III (MEp/HSi = 5/5)	98 ± 2	2H
IV (MEp/HSi = 3/7)	125 ± 2	5H
V (MEp/HSi = 1/9)	109 ± 2	6H

property of anticorrosion, it revealed maximum corrosion potential (E_{corr}) and minimum corrosion current (I_{corr}). For the hybrid coatings I, II, IV, and V, the Sea-Island morphology on the surface may weaken the barrier effect of the hybrid coatings. Besides, it should point out that excess amount of hydrolyzed TEOS may make the coating structure loose and deteriorate the anticorrosion properties, resulting in the increase of the corrosion current.

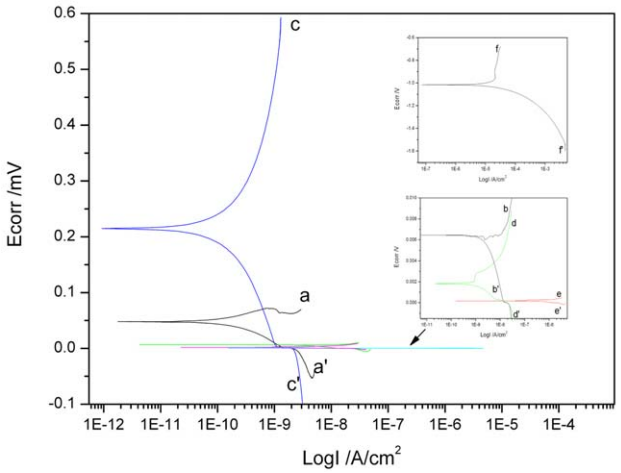

Figure 6. Potentiodynamic polarization curves of samples covered with various coatings: aa′. I(MEpHSi = 9/1); bb′. II(MEp/HSi = 7/3); cc′. III(MEp/HSi = 5/5); dd′. IV. (MEp/HSi = 3/7); ee. V(MEp/HSi = 1/9); and ff′. bare sample. [Color figure can be viewed in the online issue, which is available at wileyonlinelibrary.com.]

Table V. Electrochemical Parameters Obtained from Potentiodynamic Polarization Curves

Organic–inorganic hybrid coatings	Coating properties	
	$E(I = 0)$ (V)	I_{corr} (A)
I (MEp/HSi = 9/1)	0.048	1.77×10^{-12}
II (MEp/HSi = 7/3)	6.52×10^{-3}	4.55×10^{-11}
III (MEp/HSi = 5/5)	0.213	9.33×10^{-13}
IV (MEp/HSi = 3/7)	2.38×10^{-3}	2.28×10^{-11}
V (MEp/HSi = 1/9)	1.78×10^{-4}	1.52×10^{-10}
Bare sample	−1.015	7.44×10^{-8}

CONCLUSIONS

A series of organic–inorganic hybrid coatings were prepared by sol–gel method. These hybrid coatings were coated onto the steel panels to study the properties of water contact angles, heat resistance, pencil scratch hardness and corrosion resistance. From the observation of 3D measuring laser microscope, no cracks were present due to chemical bonding connected by the silane-coupling agent, and it present Sea-Island morphology or Inverting Sea-Island Morphology on the surface for some hybrid coatings (I, II, IV, V) which can cause the coatings present hydrophobic property. The properties of hybrid coatings varied with relative content of the two components. They present good heat resistance and high pencil scratch hardness because of the inorganic silica component. In addition, with the component of epoxy resin, the hybrid coatings show excellent anticorrosion properties. All these properties may provide us with an alternative way to substitute for the conventional chromate conversion coatings.

ACKNOWLEDGMENTS

This work was supported by JSTD Industry-University Research Cooperation Project No. BY2012178, Technology Plan Project of Hunan Province NO. 2013SK2003, and the innovative programs for Undergraduate of Jiangsu University of Science and Technology. Author also thanks Jiangsu Overseas Research & Training Program for University Prominent Young & Middle-aged Teacher and Presidents.

REFERENCES

1. Sanchez, C.; Julian, B.; Belleville, P.; Popall, M. *J. Mater. Chem.* **2005**, *15*, 3559.
2. Zheludkevich, M. L.; Miranda salvado, I.; Ferreia, M.G. S. *J. Mater. Chem.* **2005**, *15* 5099.
3. Wang, D.; Bierwagen, G. P. *J. Prog. Org. Coat.* **2009**, *64*, 327.
4. Brinker, C. J.; Scherer, J. G. W., Eds. Sol-Gel Science: The Physics and Chemicstry of Sol-Gel Processing, Academic Press: Boston **1990**; pp 787–790.
5. Williams, R. J. J.; Erra-Balsells, R.; Ishikawa, Y.; Nonami, H.; Mauri, A. N.; Riccardi, C. C. *Macromol. Chem. Phys.* **2001**, *202*, 2425.
6. Karataş, S.; Hoşg, Z.; Kayaman-Apohan, N.; Gv̈ngör, A. *Prog. Org. Coat.* **2009**, *65*, 49.
7. Yeh, J.-M.; Weng, C.-J.; Liao, W.-J.; Mau, Y.-W. *Surf. Coat. Technol.* **2006**, *201*, 1788.
8. Trabelsi, O.; Tighzert, L.; Jbara, O.; Hadjadj, A. *J. Non-Cryst. Solids* **2011**, *357*, 3910.
9. Jeevajothi, K.; Subasri, R.; Soma Raju, K. R. C. *Ceram. Int.* **2013**, *39*, 2111.
10. Feng, L.; Li, S.; Li, Y.; Li, H.; Zhang, L.; Zhai, J.; Song, Y.; Liu, B.; Jiang, L.; Zhu, D. *Adv. Mater.* **2002**, *14*, 1857.
11. Sun, C.; Ge, L. Q.; Cu, Z. Z. *Thin Solid Films* **2007**, *515*, 4686.
12. Li, H.; Wang, X.; Song, Y.; Liu, Y.; Li, Q.; Jiang, L. *Angew. Chem. Int. Ed.* **2001**, *40*, 743.
13. Xie, Q. D.; Fan, G. Q.; Zhao, N.; Guo, X. L.; Xu, J.; Dong, J. Y.; Zhang, L.Y.; Zhang, Y. J.; Han, C. C. *Adv. Mater.* **2004**, *16*, 1830.
14. Feng, L.; Li, S.; Li, H.; Zhai, J.; Song, Y.; Jiang, L.; Zhu, D. *Angew. Chem. Int. Ed.* **2002**, *41*, 1221.
15. Xie, Q. D.; Fan, G. Q.; Zhao, N.; Guo, X. L.; Xu, J.; Dong, J. Y.; Zhang, L. Y.; Zhang, Y. *J. Adv. Mater.* **2004**, *16*, 1830.
16. Lu, X. Y.; Zhang, J. L.; Zhang, C. H.; Han, Y. C. *Macromol. Rapid Commun.* **2005**, *26*, 537.
17. Erbil, H. Y.; Demirel, A. L.; Avci, Y.; Mert, O. *Science* **2003**, *229*, 1377.
18. Han, J. T.; Xu, X.; Cho, K. *Langmuir* **2005**, *21*, 6662.
19. Yabu, H.; Takebayashi, M.; Tanaka, M. *Langmuir* **2005**, *21*, 3235.
20. Najafabadi, A. H.; Mozaffarinia, R.; Rahimi, H.; Razavi, R. S.; Paimozd, E. *Prog. Org. Coat.* **2013**, *76*, 293.
21. Nadargi, D. Y.; Gurav, J. L.; El Hawi, N.; Rao, A. V.; Koebel, M. *J. Alloys Compd.* **2010**, *496*, 436.
22. Metroke, T. L.; Parkhill, R. L.; Knobbe, E. T. *Prog. Org. Coat.* **2001**, *41*, 233.
23. Campostrini, R.; Ischia, M.; Armelao, L. *J. Therm. Anal. Calorim.* **2004**, *75*, 657.
24. Zhigang, M.; Jiandong; G.; Yongjian, H. *J. Sol-Gel Sci. Technol.* **2008**, *45*, 267.
25. Mammeri, F.; Bourhis, E. L.; Rozes, L.; Sanchez, C. *J. Mater. Chem.* **2005**, *15*, 3787.
26. Conradi, M.; Kocijan, A.; Kek-Merl, D.; Zorko, M.; Verpoest, I. *Appl. Surf. Sci.* **2014**, *292*, 432.
27. Jurgen-Lohmann, D.; Nacke, C.; Simon, L.; Legge, R. *J. Sol-Gel Sci. Technol.* **2009**, *52*, 370.
28. Purcar, V.; Stamatin, I.; Cinteza, O.; Petcu, C.; Raditoiu, V.; Ghiurea, M.; Miclaus, T.; Andronie, A. *Surf. Coat. Technol.* **2012**, *206*, 4449.
29. Su, B.; Choy, K. L. *J. Mater. Sci. Lett.* **1999**, *18*, 1705.
30. Mohammad Rabea, A.; Mohseni, M.; Mirabedini, S. M.; Hashemi Tabatabaei, M. *Appl. Surf. Sci.* **2012**, *258*, 4391.